NON-EQUILIBRIUM DESCRIPTION
OF BREMSSTRAHLUNG IN DENSE MATTER
(Landau - Pomeranchuk - Migdal Effect) [1]

Jörn Knoll and Dmitri N. Voskresensky [2]

Gesellschaft für Schwerionenforschung (GSI)
Postfach 110 552
D-64220 Darmstadt, Germany

Abstract:

The soft behavior of the bremsstrahlung from a source is discussed in terms of classical transport models and within a non–equilibrium quantum field theory (Schwinger - Kadanoff - Baym - Keldysh) formulation.

Introduction

We study the importance of coherence time effects (Landau - Pomeranchuk - Migdal - effect (LPM)[3][1]) on the production and absorption of field quanta from the motion of source particles in non-equilibrium dense matter. In order to calculate such bremsstrahlung effects appropriately one needs to go beyond the commonly used quasi–particle picture, and include effects of the finite widths of the particles [2, 3, 4]. Our considerations are of particular interest for the application to photon, or di-lepton production in high energy nuclear collisions, for gluon or parton radiation and absorption in QCD transport and its practical implementation in parton kinetic models (such problems are discussed, e.g. in [4, 5]), to neutrino and axion radiation from supernovas and neutron-star matter (see [6]), for the soft phenomena in quantum cosmological gravity (see [7]) and also for many condensed matter phenomena, as particle transport in metals and semiconductors, radiation in plasma etc (see [8]). The study also gives some hints how to generalize the standard transport picture (see [9]) such that it can include genuine off-shell effects due to damping of the single particle propagation from collisions or decays.

To be specific we take the example of electrodynamics, considering photon production and assume that the source system couples only perturbatively (to lowest order) to the radiation field, while the source itself can interact in any non-perturbative way. Thus, we consider a "white" body as a source for the radiated field! Our considerations are formulated in real time non-equilibrium Green's function technique, where the production rate is given by the $-+$ component of the proper self-energy diagram of the produced

---

[1] *GSI-preprint 95-18; submitted to Phys. Lett. B*

[2] permanent adress: Moscow Institute for Physics and Engineering, Russia, 115409 Moscow, Kashirskoe shosse 31

[3] The original LPM considerations were restricted to cases where ultra-relativistic particles traverse a finite piece of target matter.

photon

$$-\mathrm{i}\Pi^{-+} = \;\overset{+}{\cdots}\!\!\left(\!\!-\mathrm{i}\boldsymbol{\Pi}\!\!\right)\!\!\overset{-}{\cdots} = 4\pi \int d^4\xi e^{\mathrm{i}q\xi} \left\langle j^{\nu\dagger}(x-\xi/2)j^{\mu}(x+\xi/2)\right\rangle,\tag{1}$$

which is determined by the current auto correlation function of the source. The dashed lines relate to the photon, while the $-\mathrm{i}\Pi$-loop symbolically denotes the exact inclusion of all strong interaction among the source particles. The bracket $\langle\ldots\rangle$ denotes a quantum ensemble average over the source with quantum states and operators in the interaction picture. Above and throughout later we use the Keldysh $\{-,+\}$ notation, see [10], where the Π^{-+} and Π^{+-} self energies are responsible for gain and loss. Such a formalism has been applied in calculation of neutrino emissivity of neutron stars in ref.[11], employing the quasi–particle approximation for the equilibrium nucleon Green functions. However the general formalism allows to go beyond this limit and to account for the finite damping width of the source particles due to their finite mean free path.

Classical radiation

For some classical source systems perturbatively coupled to a boson field the boson self energy can be obtained in closed form. For these cases one has to evaluate the current-current correlator on the classical level. The properties of classical radiation will be illustrated for two examples, where a charged particle (the source) stochastically moves in dense matter. Thereby the motion of the charge is described either (a) by mesoscopic transport (diffusion process) or (b) by a microscopic Langevin process.

Diffusion process

The motion of the source particle is assumed to be described by a time dependent phase-space distribution $f(\vec{x},\vec{v},t)$ in space and velocity with convective current density $\vec{j}(\vec{x},t) = e\int d^3v \; \vec{v} \; f(\vec{x},\vec{v},t)$. For standard dissipative media in equilibrium the velocity autocorrelation function (integrated over space) decays exponentially in time[4]

$$\left\langle v^i(\tau)v^k(0)\right\rangle = \frac{1}{3}\left\langle\vec{v}^2\right\rangle \delta^{ik} e^{-\Gamma_x|\tau|},\tag{2}$$

where i and j denote the spatial components. Γ_x is the relaxation rate which we approximate as constant, $\langle\ldots\rangle$ now denotes the average over the classical distribution functions.

Both $f(\vec{x},\vec{v},t)$ and the autocorretion function can be obtained in closed form, if the time evolution of f, and the propagation of fluctuations δf are governed by a standard diffusion process. Solving then a *Fokker-Planck* equation for the space-time dependence of velocity fluctuations we obtain (in mixed $\tau,\vec{q}$ representation)

$$
\begin{aligned}
-\mathrm{i}\Pi_{\mathrm{cl}}^{-+}(\tau,\vec{q}) &= 4\pi \int d^3\vec{x}\, e^{-\mathrm{i}\vec{q}\vec{x}} \left\langle j^i(\vec{x},\tau)j^k(\vec{0},0)\right\rangle \\
&= 4\pi e^2\rho_0 \left\{ \left\langle\!\left\langle v^i v^k\right\rangle\!\right\rangle_{eq} e^{-\Gamma_x|\tau|} - D^2 q^i q^k \left(e^{-\Gamma_x|\tau|}-1\right)^2 \right\} \\
&\quad \times \exp\left\{ -\frac{D\,\vec{q}^2}{\Gamma_x}\left(\Gamma_x|\tau| + e^{-\Gamma_x|\tau|} - 1\right)\right\}.
\end{aligned}\tag{3}
$$

---

[4]We should note that this ansatz ignores finite size corrections in terms of some anti-correlations on the scale of a mean recurrence time [3].

Here the ensemble average $\langle\ldots\rangle_{eq}$ over the equilibrium distribution f_{eq} keeps only even moments of $\vec{v}$ with $\langle\vec{v}^2\rangle = 3D\Gamma_x$ such that only even powers of $i\vec{q}$ survive. This renders $-i\Pi_{\text{cl}}^{-+}(\tau,\vec{q})$ real and symmetric in τ. For transverse photons $\vec{\eta}\vec{q} = 0$ some terms drop and we have

$$
\begin{aligned}
-i\Pi_{\text{cl}}^{-+}(\omega,\vec{q}) \ &= 4\pi e^2 \rho_0 \left\langle v^i v^j \right\rangle_{eq} \exp\left[D\,\vec{q}^2/\Gamma_x\right] \\
&\times \sum_{k=0}^{\infty} \frac{1}{k!}\left(\frac{-D\,\vec{q}^2}{\Gamma_x}\right)^k \frac{2(k+1)\Gamma_x + 2D\,\vec{q}^2}{\left((k+1)\Gamma_x + D\,\vec{q}^2\right)^2 + \omega^2} \quad (4) \\
&\longrightarrow 4\pi e^2 \rho_0 \left\langle v^i v^j \right\rangle_{eq} 2\Gamma_x/(\omega^2 + \Gamma_x^2) \quad \text{for} \quad \langle v^2\rangle\vec{q}^2 \ll \Gamma_x^2. \quad (5)
\end{aligned}
$$

Compared to the infra–red divergent quasi–free result $\propto 1/\omega^2$ this form of the correlation renders the photon self energy regular in the soft limit at four momentum $q = 0$. It is determined by mesoscopic transport properties, namely by the relaxation rate Γ_x and the diffusion coefficient $D = \langle\vec{v}^2\rangle /3\Gamma_x$; ρ_0 is the spatial density of the charged particles. For large q, i.e. $Dq^2 \gg \Gamma_x$, only the short time behavior of the autocorrelation matters and from (3) and (4) one finds in $(\tau,\vec{q})$ and $(\omega,\vec{q})$ representations

$$
\lim_{D\,\vec{q}^2 \gg \Gamma_x} \left[-i\Pi_{\text{cl}}^{-+}(\tau,\vec{q})\right] = 4\pi e^2 \rho_0 \left\langle v^i v^k \right\rangle_{eq} \exp\left[-\Gamma_x|\tau| - D\,\vec{q}^2\Gamma_x\tau^2/2\right], \quad (6)
$$

$$
\lim_{D\,\vec{q}^2 \gg \Gamma_x} \left[-i\Pi_{\text{cl}}^{-+}(\omega,\vec{q})\right] = 4\pi e^2 \rho_0 \left\langle v^i v^k \right\rangle_{eq} \left(\frac{2\pi}{D\,\vec{q}^2\Gamma_x}\right)^{3/2} \exp\left\{-\frac{\omega^2}{2D\,\vec{q}^2\Gamma_x}\right\}. \quad (7)
$$

Microscopic Langevin process

In a *microscopic Langevin* process hard scatterings occur at random with a constant mean collision rate Γ. These scatterings consecutively change the velocity of a point charge from $\vec{v}_m$ to $\vec{v}_{m+1},\ldots$ (subscripts m, and n below refer to the collision sequence). In between scatterings the point charge moves freely. For such a multiple collision process one can at least determine the $\vec{q} = 0$ part of the self energy.

The modulus of the autocorrelation function takes a Poissonian form for such a collision sequence

$$
-i\Pi_{\text{cl}}^{-+}(\tau,\vec{q} = 0) = 4\pi e^2 \rho_0 \left\langle v^i(\tau)v^k(0)\right\rangle = 4\pi e^2 \rho_0 e^{-|\Gamma\tau|} \sum_{n=0}^{\infty} \frac{|\Gamma\tau|^n}{n!} \left\langle v_m^i v_{m+n}^k \right\rangle_m, \quad (8)
$$

where $\langle\ldots\rangle_m$ denotes the average over the discrete collision sequence $\{m\}$. The time Wigner transform of (8) determines the spectrum at vanishing $\vec{q}$ for all ω

$$
-i\Pi_{\text{cl}}^{-+}(\omega,\vec{q} = 0) = 4\pi e^2 \rho_0 \sum_{n=0}^{\infty} \left\langle v_m^i v_{m+n}^j \right\rangle_m \frac{2\Gamma^n \text{Re}\left\{(\Gamma + i\omega)^{n+1}\right\}}{(\omega^2 + \Gamma^2)^{n+1}}. \quad (9)
$$

This is a genuine *multiple collision* description for the photon production rate in completely regular terms due to the $(\omega^2 + \Gamma^2)^n$ form of all denominators. Each term is regular, since right from the beginning one accounts for the damping of the source particle because of the finite mean time $1/\Gamma$ between collisions. The result (9) still accounts for the *coherence* of the photon field, now expressed through the correlations $\langle\vec{v}_m\vec{v}_{m+n}\rangle_m$ arizing

3

from the sequence of collisions. The terms in (9) define partial rates, which are associated with specific self energy diagrams.

For the Langevin process the $\vec{q}$-dependence of the self energy cannot be obtained in closed form in general. Still the $n = 0$ term (c.f. with $n = 0$ term from eq.(9)) can be given

$$- i\Pi_{cl}^{-+}(\omega, \vec{q}) \approx 4\pi e^2 \rho_0 \left\langle \frac{2\Gamma \, v_m^i v_m^k}{(\omega - \vec{q}\vec{v})^2 + \Gamma^2} \right\rangle_m . \tag{10}$$

It shows the typical Cherenkov enhancement at $\omega = \vec{q}\vec{v}$. Although for $\vec{q} \to 0$ the analytical form of (10) resembles the diffusion result (4), it is not the same unless $\langle \vec{v}_m \, \vec{v}_{m+n} \rangle_m = 0$ for $n \neq 0$, an approximation recently used in ref. [12]. In the general case velocity correlations between successive scatterings exist, and there will be a sizeable difference between the microscopic mean collision rate Γ and the mesoscopic relaxation rate Γ_x. For systems, where the velocity is degraded by a constant fraction α, such that $\langle \vec{v}_m \cdot \vec{v}_{m+n} \rangle_m = \alpha^n \langle \vec{v}_m \cdot \vec{v}_m \rangle_m$, one can sum up the whole series in (9) and recover the diffusion result (4) at $\vec{q} = 0$ with $\Gamma_x = (1 - \alpha)\Gamma$. This clarifies that the diffusion result (4) represents a resummation of the random multiple collision result (9).

Monte Carlo evaluation of amplitudes

Some of the cascade schemes try to cure the infra-red problem by considering the phase of the photon field along the classical orbits. Thus they evaluate $\int \mathrm{d}t \vec{v}(t) \exp[i\omega t - i\vec{q}\vec{x}(t)]$ along the random straight sections of the classical paths in the cascade model. We like to mention that this is a highly unreliable procedure due to the strong cancelations of terms that are randomly generated. Our experience shows that a reliable result (better than $< 5\%$) in the transition region $\omega \approx \Gamma$ requires an ensemble of 10^3 cascade runs where each path has about 10^3 collisions. Compared to that the analytical result (9) has significant computational advantages, provided the random process is of this form.

Quantum many-body description

In the full quantum field theory formulation the production rate is given by all photon self energy diagrams of skeleton type according to the closed time-path rules [10, 13] with *full* Green's function which result from the summation of Dyson's equation. The later in short matrix notation becomes

$$\boldsymbol{G} = \boldsymbol{G}_0 + \boldsymbol{G}_0 \odot \boldsymbol{\Sigma} \odot \boldsymbol{G} \tag{11}$$
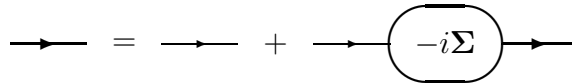
Here $\boldsymbol{G}_0$, $\boldsymbol{G}$ and $\boldsymbol{\Sigma}$ denote the two by two matrices of the unperturbed Green's function (thin lines), the full Green's function (full lines), and the proper self energy of the source particles. The $\odot$ denotes the space-time folding. The four components of $-i\boldsymbol{\Sigma}$ are defined as the sum of all standard proper self energy diagrams like in normal perturbation theory, now however with definite $+$ or $-$ assignments at the external vertices, and summed over the $-$ and $+$ signs for all internal vertices. These signs specify the Green's functions linking the vertices and the choice between the $-$ vertex $-iV$ and its adjoint value $+iV^\dagger$ at $+$ vertices (c.f. ref. [10]).

The full Green's functions account for the finite damping width of the particles, and therefore destroy of the strict energy-momentum relation in dense matter. This width expressed through the imaginary part $-\Gamma$ of the retarded self energy arises from collisions or decays of the particles. In this picture the off-diagonal Green's functions G^{-+} and G^{+-} are *four momentum and space Wigner densities* for the occupied and available 'single particle states', which now have a finite width. The corresponding off-diagonal parts in the self energy determine the corresponding gain and loss terms in a transport description. Therefore each diagram of (1) defines a specific partial rate.

We suggest a decomposition of the diagrams that allow for a simple interpretation and classification in terms of physical in-medium scattering processes, and propose particular resummations of physically meaningful diagrams, which consider the finite damping width of all source particles in matter. All the graphs consisting $G^{-+}G^{+-}$–products are explicitly presented. In this picture the set of diagrams reduces to

$$\tag{12}$$

Here full dots and boxes denote effective in-medium vertices and 4-point interactions, e.g.

$$\tag{13}$$

These in-medium vertices and four point interactions are defined for a specific choice of sign (say $-$) through skeleton resummation schemes, where only bare $-$ vertices linked by G^{--} Green's functions appear. Compared to conventional diagrams, vertex corrections of different signs appear on both sides of a loop once they are separated by $\{+-\}$ lines. In (13) the wavy lines are either interactions or full boson-propagators in a theory of fermions interacting with bosons, like in QCD. In some simplified representations (being often used, c.f. [11]) the 4-point functions behave like intermediate bosons (e.g. phonons).

We note that each diagram in (12) represents already a whole class of perturbative diagrams of any order in the interaction and in the number of loops. The most essential term is the one-loop diagram in (12), which is positive definite, and corresponds to the first term of the classical Langevin result for Π_{cl} in (9). The other diagrams represent interference terms due to rescattering. All diagrams calculated with full Green's functions are void of infra-red divergences. Thus these diagrams represent the quantum generalization of the infra-red regular Langevin result (9). Under appropriate conditions, the correct *quasi–particle* (QP) and *quasi–classical* (QC) limits are recovered from this subset of graphs.

Decomposition of closed diagrams into Feynman amplitudes in the quasi–particle approximation (QPA)

The QPA is a quite commonly used concept originally derived for Fermi liquids at low temperature (Landau - Migdal, see [14]), where it constitutes a consistent scheme. With

the application of transport models to high energy situations this concept has been taken over to a regime where its validity cannot be justified under all circumstances. For the validity of the QPA one normally assumes that $\Gamma \ll \bar{\epsilon}$, where $\bar{\epsilon}$ is an average particle kinetic energy ($\sim T$ for equilibrium matter). This has considerable computational advantages as Wigner densities (" $-+$ " and " $+-$ " lines) become energy δ–functions, and the particle occupations can be considered to depend on momentum only rather than on the energy variable.[5]. Formally the energy integrals can be eliminated, in diagrammatic terms just cutting the corresponding " $-+$ " and " $+-$ " lines [11].

Thus the QP picture allows a transparent interpretation of closed diagrams. With consecutive numbers 1 to 6 for the diagrams drawn in (12), diagrams 1, 2, 4 and 5 relate to the radiation from a single in-medium scattering between two fermionic quasi-particles [15]. Thereby diagram 2 is more important than diagram 4 for neutral interactions, while this behavior reverses for charge exchange interactions (the latter is also important for gluon radiation in QCD transport due to color exchange interactions). Diagrams like 3 describe the interference terms due to further rescatterings of the source fermion with others. For diagram 6 the photon is produced from intermediate states (its contribution is suppressed in the soft limit). Some of the diagrams, which are not presented explicitly in eq.(12) give more than two pieces, if cut, so they do not reduce to the Feynman amplitudes. Since one works with zero-width fermion Green's functions in QPA, the finite width contributions have to appear in higher order diagrams through corresponding **Im**Σ-insertions! Therefore the whole set of diagrams defining the full $-i\Pi^{-+}$ in QPA is by far larger, than ours (12).

Moreover, our considerations show that the validity condition $\Gamma \ll \bar{\epsilon}$ is not sufficient for the QPA. Rather, since finally energy differences of order ω appear, one has to demand that also $\omega \gg \Gamma$ in the QPA. In particular, the remaining series of QP-diagrams is *no longer convergent* unless $\omega > \Gamma$, since arbitrary powers in Γ/ω appear, and there is no hope to ever recover a reliable result by a finite number of QP-diagrams for the production of soft quanta! With *full Green's functions*, however, one obtains a description that uniformly covers both, the soft ($\omega \ll \Gamma$) and the hard ($\Gamma \ll \omega$) regime.

Quasi-classical limit (QCL)

The QCL requires that *i*) the particle occupations are small ($\langle n_{\vec{p}} \rangle \ll 1$) implying a Boltzmann gas and that *ii*) all inverse length or time-scales times $\hbar$ are small compared to the typical momentum and energy scales of the source systems. In particular we shall assume $\hbar\omega \ll \bar{\epsilon}$, and a fermion collision rate $\Gamma = \hbar/\tau_{\text{coll}} \ll \bar{\epsilon}$. The last inequality allows to use Kadanoff–Baym ansatz, where the fermion occupations depend only on momentum $n_{\vec{p}} = n_{\epsilon_{\vec{p}} - \mu_F}$ but no longer on the energy ϵ of the particles. Assuming again $\Gamma \simeq const.$ on relevant time scales one immediately finds

$$G^{-+}(\tau, \vec{p}) \simeq i n_{\vec{p}} \exp[-|\Gamma\tau|/2 + i\epsilon_{\vec{p}}\tau], \tag{14}$$

$$G^{+-}(\tau, \vec{p}) \simeq -i(1 - n_{\vec{p}}) \exp[-|\Gamma\tau|/2 - i\epsilon_{\vec{p}}\tau]. \tag{15}$$

With these Green functions we calculate the diagrams (12). For the one–loop diagram we

---

[5]The later approximation is also often used beyond the scope of the QPA and is then known as Kadanoff–Baym ansatz [13], c.f.[8]

obtain the expression identical to the $n = 0$ term of the classical Langevin result (10):

$$- i\Pi_0^{-+}(\omega, \vec{q}) \approx 4\pi e^2 \int \frac{d^3 p}{(2\pi)^3} \frac{n_{\vec{p}}(1 - n_{\vec{p}}) 2\Gamma v^i v^k}{(\omega - \vec{q}\vec{v}))^2 + \Gamma^2} \approx 4\pi e^2 \rho_0 \left\langle \frac{2\Gamma v^i v^k}{(\omega - \vec{q}\vec{v}))^2 + \Gamma^2} \right\rangle . \quad (16)$$

For neutral interactions (corresponding to the classical examples) we show that precisely the diagrams in the first line of (12) denoted by $-i\Pi_n^{-+}$ with n $\{-+\}$ loop insertions correspond to the n-th term of the Langevin result (9)[6]. Thus

$$- i\Pi_n^{-+}(\tau, \vec{q} = 0) \approx 4\pi e^2 \rho_0 \left\langle v_m^i v_{m+n}^k \right\rangle_m \frac{|\Gamma\tau|^n}{n!} e^{-|\Gamma\tau|}, \quad (17)$$

$$- i\Pi_n^{-+}(\omega, \vec{q} = 0) \approx 4\pi e^2 \rho_0 \left\langle v_m^i v_{m+n}^k \right\rangle_m 2\Gamma^n \mathbf{Re} \frac{1}{(\Gamma - i\omega)^{n+1}}. \quad (18)$$

For neutral interactions all other diagrams in (12) drop in the QC limit. Diagram 4 is unimportant for neutral interactions. Other diagrams in the original series (12) acquire extra powers either in the mean occupation $\langle n_{\vec{p}} \rangle \ll 1$ or in $\Gamma/\bar{\epsilon} \ll 1$. Such suppression factors result from extra G^{-+} lines compared to the classical diagrams of the same topology or are due to a violation of time ordering (diagram 5), since classical interactions are of time-scale $1/\bar{\epsilon}$, which is short compared to the damping time $1/\Gamma_x$.

We note that truncating the set of diagrams (12) with respect to a certain expansion parameter special care should be taken in order to satisfy charge–current conservation law. For verification one may use the Ward–Takahashi identities within the desired order.

For equilibrium $T \neq 0$ case even in general quantum consideration the one–loop diagram can be expressed by the QP prescription [11, 15] however multiplied by the factor $C = \omega^2/(\omega^2 + \Gamma^2)$, which displays the suppression at low ω. There is hope that even in the quantum case some higher order diagrams can also be resummed and that an overall suppression factor of the form $C = \omega^2/(\omega^2 + \Gamma_x^2)$ emerges for the true in-matter rate relative to the quasi-free or QP one in the limit $q = 0$, c.f. the diffusion result (3-7).

Altogether our results provide an extension of the *incoherent quasi–free* and QP approximation from the ultra violet limit towards the soft limit with appropriately modified production cross sections. It does not only regularize the infra–red divergence of the free rate, but it also produces the right q dependence in the soft limit. We also note that our diagrammatic description may suggest a formulation of a transport theory which includes the propagation of particles with finite width and therefore may permit a consistent treatment of resonances in non–equilibrium dense matter.

---

[6]The proof is easily given in the $\tau - \vec{p}$ representation, assigning times 0 and τ to the external $-$ and $+$ vertices, while the internal $-$ and $+$ vertices are taken at t_1^- to t_n^- and t_1^+ to t_n^+, respectively. In the classical limit G^{--} is retarded, while G^{++} is advanced, such that both time sequences have the same ordering: $0 < t_1^- < \ldots < t_n^- < \tau$ and $0 < t_1^+ < \ldots < t_n^+ < \tau$ (the order reverses, if the line sense of the outer fermion lines are reversed). Thus the τ-dependence of the modulus of these diagrams again results in $e^{-|\Gamma\tau|}$. Assuming classical momentum transfers $|\vec{p}_n - \vec{p}_{n+1}|$ which are large compared to $\hbar\Gamma$ one concludes that the $\{+-\}$ loop insertions merge $\delta(t_n^- - t_n^+)$ in their time structure. With $t_n = t_n^- = t_n^+$ a given diagram then no longer depends on the intermediate times t_n apart from the ordering condition, and therefore results in a factor $|\Gamma\tau|^n/n!$. With $\vec{q} = 0$ also the corresponding momenta are pair-wise identical, and the remaining momentum integrations just serve to define the correlation between $\vec{v}_m$ and $\vec{v}_{m+n}$ after n collisions of the charged particle.

References

[1] L. D. Landau and I. Pomeranchuk, Dokl. Akad. Nauk SSSR **92** (1953) 553, 735; also in Coll. Papers of Landau, ed. Ter Haar (Gordon & Breach, 1965) papers 75 - 77; A. B. Migdal, Phys. Rev. **103**, (1956)1811; Sov. Phys. JETP **5** (1957) 527

[2] J. Knoll and C. Guet, Nucl. Phys. **A494** (1989) 334; M. Durand and J. Knoll, Nucl. Phys. **A496** (1989) 539;

[3] J. Knoll and R. Lenk, Nucl. Phys. **A 561** (1993) 501

[4] J. Cleymans, V.V. Goloviznin, and K. Redlich, Phys. Rev.**D47** (1993) 989; X. N. Wang and M. Gyulasssy, Nucl. Phys. **B 420** (1994) 583; R. Baier, Yu. L. Dokshitzer, S. Reigne and D. Schiff, Bielefeld BI-TP 94/57; P. A. Henning and R. Sollacher, preprint, GSI-95-04

[5] Proceedings of the Tenth International Conference on Ultra–Relativistic Nucleus–Nucleus Collisions, eds: E. Stenlund, H. –A. Gustafsson, A.Oskarsson and I.Otterlund (North–Holland, 1994); Nucl.Phys. **A566**, 1c (1994)

[6] Neutron Stars, ed. by D. Pines, R. Tamagaki and S. Tsuruta, Addison–Weseley, N. Y. (1992) G. Raffelt and D. Seckel, MPI-Ph/93-90

[7] N. S. Tsamis and R. P. Woodard, Ann. Phys. (N. Y.) **238** (1995) 1

[8] V. Spicka and P. Lipavsky, Phys. Rev. Lett. **73** (1994), 3439; P. Lipavsky,V. Spicka and B. Velicky, Phys. Rev. **B34** (1986), 6933

[9] P. Danielewicz, Ann. Phys. (N. Y.) **152** (1984) 239, 305; P. Danielewicz and G. Bertsch, Nucl. Phys. **A533** (1991) 712

[10] c.f. E. M. Lifshiz and L. P. Pitaevskii, Physical Kinetics (Nauka, 1979); Pergamon press (1981)

[11] D. N. Voskresensky and A. V. Senatorov, Yad. Fiz. **45** (1987) 657; in Engl. translation Sov.J.Nucl.Phys.**45** (1987) 411

[12] J. Cleymans, V.V. Goloviznin, and K. Redlich, Phys. Rev.**D47** (1993) 173

[13] L. P. Kadanoff and G. Baym, Quantum Statistical Mechanics (Benjamin, 1962)

[14] E. M. Lifshiz and L. P. Pitaevskii, Statistical Physics, p.2 (Nauka, 1978); Pergamon press (1980); A. B. Migdal, Theory of Finite Fermi Systems and Properties of Atomic Nuclei , Willey and sons, 1967, Nauka; 1983

[15] D. N. Voskresensky and A. V. Senatorov, Yad. Fiz. **52** (1990) 447; in Engl. translation Sov.J.Nucl.Phys.**52** (1990) 284